

IPST2025

International Conference on
Power Systems Transients
Guadalajara, México.
8 to 12 June, 2025

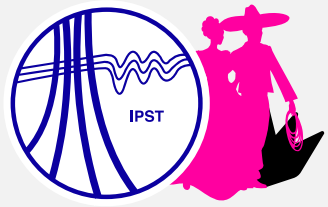
Sustained Oscillations of Grid-forming IBRs under Unbalanced Perturbation: Modal Analysis and EMT Studies

Xinquan Chen, Tao Xue, Ilhan Kocar, Siqi Bu, Maxime Berger

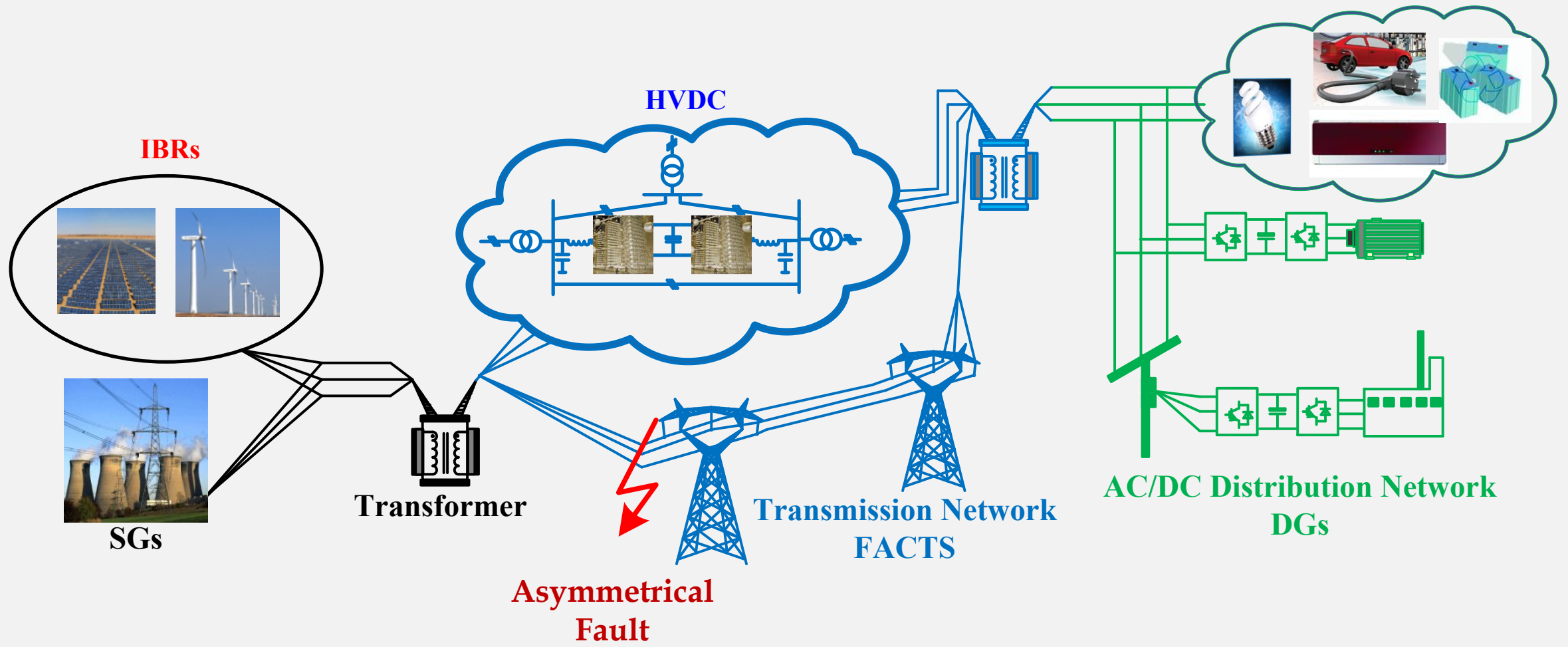
Presenter: Prof. Ilhan Kocar

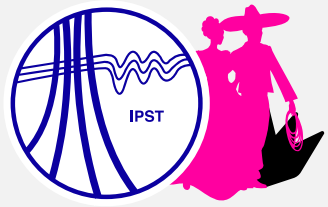
Polytechnique Montreal
ilhan.kocar@polymtl.ca

June 8, 2025

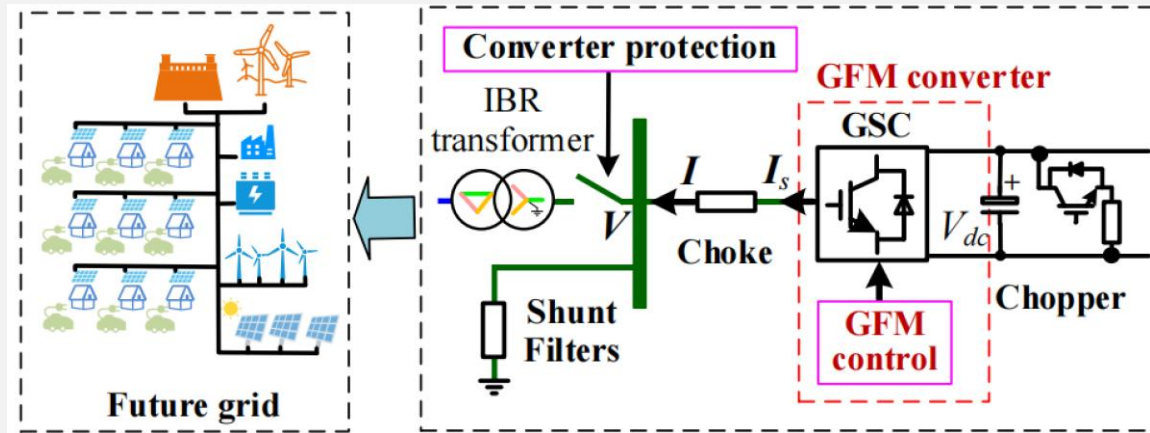


1. Introduction





1. Introduction



Grid-forming inverter-based resources (GFM-IBRs) are considered crucial for power systems with high penetration renewable energy, but their negative sequence behavior under small perturbations remains understudied.

- Develop a decoupled-sequence modeling approach for GFM-IBRs that incorporates double-fundamental-frequency (2ω) negative-sequence components.
- Analyze the oscillatory modes of GFM-IBRs in the negative-sequence system using modal analysis and EMT studies.
- Evaluate the effectiveness of additional negative sequence control strategies in improving system damping.

2. Oscillation under Unbalanced Perturbation

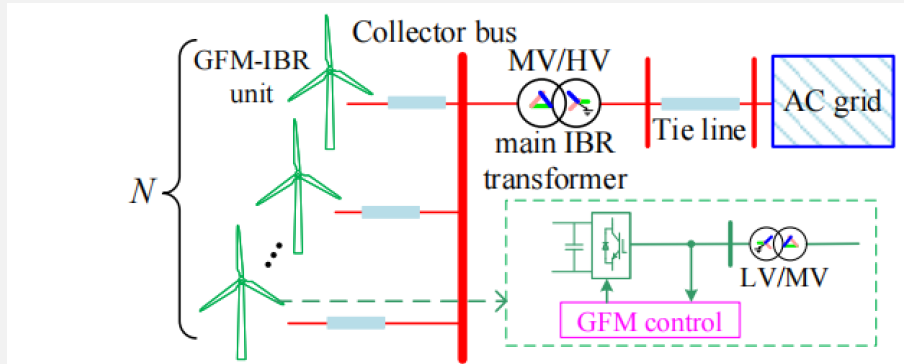


Fig. 1. GFM-IBR plant in power systems

Unbalanced AC
grid conditions

$$\mathbf{X}_{dq} = \begin{bmatrix} X_\alpha \cos(\theta) + X_\beta \sin(\theta) \\ X_\beta \cos(\theta) - X_\alpha \sin(\theta) \end{bmatrix}$$

$$= \mathbf{X}_{dq}^+ + \begin{bmatrix} X_d^- \cos(2\omega t) + X_q^- \sin(2\omega t) \\ X_q^- \cos(2\omega t) - X_d^- \sin(2\omega t) \end{bmatrix} = \mathbf{X}_{dq}^+ + \tilde{\mathbf{X}}_{dq}^-$$

- Under unbalanced perturbations, positive-, negative- and zero-sequence components of both voltages and currents are typically present in the AC grid.
- 2ω components exist in the control loop

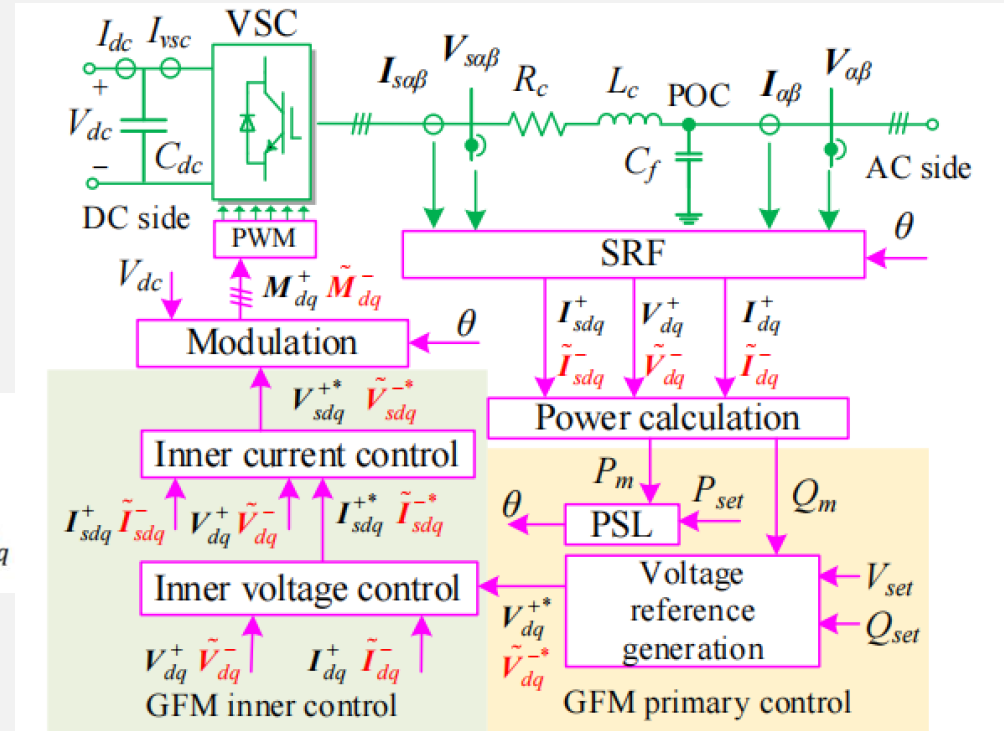
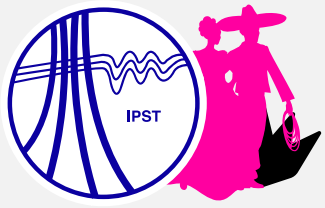


Fig. 2. Sequence components within the typical GFM BPSC system under unbalanced perturbations



3. Decoupled-Sequence Dynamic Modelling for GFM-IBRs

GFM primary control:

VSM control

$$\begin{cases} \dot{\omega} = \frac{(P_{set} - x_P)}{J\omega_n} + \frac{D_p(\omega_n - \omega)}{J} \\ \dot{x}_P = \omega_f(P_m - x_P) \end{cases}$$

$$V_d = V_d^+ + \tilde{V}_d^- = V_d^+ + V_d^- \cos(2\omega t) + V_q^- \sin(2\omega t)$$

$$\psi_M = \psi_M^+ + \tilde{\psi}_M^-$$

$$\begin{cases} \psi_M^+ = k_{pvac} \underbrace{(V_{set} - V_d^+)}_{\dot{x}_V^+} + k_{ivac} \dot{x}_V^+ \\ \tilde{\psi}_M^- = k_{pvac} \underbrace{(0 - \tilde{V}_d^-)}_{\dot{\tilde{x}}_V^-} + k_{ivac} \dot{\tilde{x}}_V^- \end{cases}$$

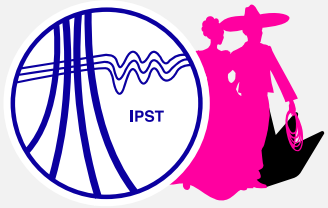
$$\begin{cases} V_{dq}^{+*} = \mathbf{T}_{dq}(\theta) \mathbf{T}_{\alpha\beta} \omega \psi_M^+ \sin(\hat{\theta}) \\ \tilde{V}_{dq}^{-*} = \mathbf{T}_{dq}(\theta) \mathbf{T}_{\alpha\beta} \omega \tilde{\psi}_M^- \sin(\hat{\theta}) \\ \sin(\hat{\theta}) = \left[\sin(\theta) \quad \sin(\theta - \frac{2\pi}{3}) \quad \sin(\theta - \frac{4\pi}{3}) \right]^T \end{cases}$$

droop control

$$\begin{aligned} \omega &= \omega_n - m_p(P_m - P_{set}) \\ \begin{cases} V_d^* = V_d^{+*} + \tilde{V}_d^{-*} \\ V_q^* = 0 \end{cases} &\begin{cases} V_d^{+*} = k_{pvac} \underbrace{(V_{set} - V_d^+)}_{\dot{x}_V^+} + k_{ivac} \dot{x}_V^+ \\ \tilde{V}_d^{-*} = k_{pvac} \underbrace{(0 - \tilde{V}_d^-)}_{\dot{\tilde{x}}_V^-} + k_{ivac} \dot{\tilde{x}}_V^- \end{cases} \end{aligned}$$

dVOC

$$\begin{aligned} \begin{cases} \omega &= \omega_n + \kappa_1 \left(\frac{P_{set}}{(V_{set})^2} - \frac{x_P}{(V_d^*)^2} \right) \\ \dot{x}_P &= \omega_f(P_m - x_P) \end{cases} \\ \begin{cases} \dot{V}_d^* &= V_d^* \left(\kappa_1 \left(\frac{Q_{set}}{(V_{set})^2} - \frac{x_Q}{(V_d^*)^2} \right) + \frac{\kappa_2(V_{set}^2 - (V_d^*)^2)}{V_{set}^2} \right) \\ \dot{x}_Q &= \omega_f(Q_m - x_Q) \end{cases} \end{aligned}$$



3. Decoupled-Sequence Dynamic Modelling for GFM-IBRs

GFM inner control:

$$\mathbf{X} = \{I, V, I_s\}$$

$$\mathbf{X}_{dq} = \mathbf{X}_{dq}^+ + \tilde{\mathbf{X}}_{dq}^- = \begin{bmatrix} X_d^+ + X_d^- \cos(2\omega t) + X_q^- \sin(2\omega t) \\ X_q^+ + X_q^- \cos(2\omega t) - X_d^- \sin(2\omega t) \end{bmatrix}$$

$$\begin{cases} I_{sdq}^{+*} = k_{iv} \mathbf{x}_{vdq}^+ + k_{pv} \underbrace{(\mathbf{V}_{dq}^{+*} - \mathbf{V}_{dq}^+)}_{\hat{\mathbf{x}}_{vdq}^+} + \underbrace{\gamma C_f \mathbf{V}_{dq}^+ + I_{dq}^+}_{\text{feedforward}} \\ \tilde{I}_{sdq}^{-*} = k_{iv} \tilde{\mathbf{x}}_{vdq}^- + k_{pv} \underbrace{(\tilde{\mathbf{V}}_{dq}^{-*} - \tilde{\mathbf{V}}_{dq}^-)}_{\hat{\tilde{\mathbf{x}}}_{vdq}^-} + \underbrace{\gamma C_f \tilde{\mathbf{V}}_{dq}^- + \tilde{I}_{dq}^-}_{\text{feedforward}} \end{cases}$$

$$\begin{cases} \mathbf{V}_{sdq}^{+*} = k_{pi} \underbrace{(\mathbf{I}_{dq}^{+*} - \mathbf{I}_{dq}^+)}_{\hat{\mathbf{x}}_{ldq}^+} + k_{ii} \mathbf{x}_{ldq}^+ + \underbrace{\gamma L_c \mathbf{I}_{dq}^+ + \mathbf{V}_{dq}^+}_{\text{feedforward}} \\ \tilde{\mathbf{V}}_{sdq}^{-*} = k_{pi} \underbrace{(\tilde{\mathbf{I}}_{dq}^{-*} - \tilde{\mathbf{I}}_{dq}^-)}_{\hat{\tilde{\mathbf{x}}}_{ldq}^-} + k_{ii} \tilde{\mathbf{x}}_{ldq}^- + \underbrace{\gamma L_c \tilde{\mathbf{I}}_{dq}^- + \tilde{\mathbf{V}}_{dq}^-}_{\text{feedforward}} \end{cases}$$

$$\begin{cases} \mathbf{M}_{dq}^+ = \frac{2}{V_{dc}} \mathbf{V}_{sdq}^{+*} \\ \tilde{\mathbf{M}}_{dq}^- = \frac{2}{V_{dc}} \tilde{\mathbf{V}}_{sdq}^{-*} \end{cases} \quad \mathbf{M}_{dq}^- = \begin{bmatrix} \tilde{M}_d^- \cos(2\omega t) - \tilde{M}_q^- \sin(2\omega t) \\ \tilde{M}_q^- \cos(2\omega t) + \tilde{M}_d^- \sin(2\omega t) \end{bmatrix}$$

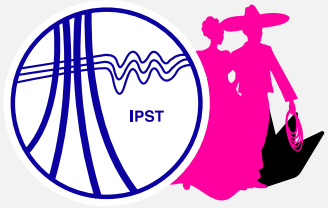
GFM PNSC System

Balanced voltage control strategy:

$$\begin{cases} \mathbf{V}_{dq}^{-*} = 0 \\ I_{sdq}^{-*} = (k_{pv} + \frac{k_{iv}}{s})(\mathbf{V}_{dq}^{-*} - \mathbf{V}_{dq}^-) + \gamma C_f \mathbf{V}_{dq}^- + I_{dq}^- \\ \mathbf{V}_{sdq}^{-*} = (k_{pi} + \frac{k_{ii}}{s})(I_{sdq}^{-*} - I_{sdq}^-) + \gamma L_c I_{sdq}^- + \mathbf{V}_{dq}^- \\ \mathbf{M}_{dq}^- = \frac{2}{V_{dc}} \mathbf{V}_{sdq}^{-*} \end{cases}$$

Balanced current control strategy:

$$\begin{cases} I_{sdq}^{-*} = 0 \\ \mathbf{V}_{sdq}^{-*} = (k_{pi} + \frac{k_{ii}}{s})(I_{sdq}^{-*} - I_{sdq}^-) + \gamma L_c I_{sdq}^- + \mathbf{V}_{dq}^- \\ \mathbf{M}_{dq}^- = \frac{2}{V_{dc}} \mathbf{V}_{sdq}^{-*} \end{cases}$$



3. Decoupled-Sequence Dynamic Modelling for GFM-IBRs

AC and DC systems

$$\begin{cases} I_{dcset} = k_{Vdc}(V_{dcset} - V_{dc}) \\ \dot{I}_{dc} = \frac{I_{dcset} - I_{dc}}{T_{dc}} \\ \dot{V}_{dc} = \frac{I_{dc} - I_{vsc}}{C_{dc}} = \frac{I_{dc} - \frac{1}{2}(\mathbf{M}_{\alpha\beta})^T \mathbf{I}_{\alpha\beta}}{C_{dc}} \end{cases}$$

$$\begin{cases} \dot{\mathbf{i}}_{sdq}^+ = \frac{\mathbf{v}_{sdq}^+ - R_c \mathbf{I}_{sdq}^+ - \mathbf{v}_{dq}^+}{L_c} + \boldsymbol{\gamma} \mathbf{I}_{sdq}^+ \\ \dot{\mathbf{i}}_{sdq}^- = \frac{\mathbf{v}_{sdq}^- - R_c \mathbf{I}_{sdq}^- - \mathbf{v}_{dq}^-}{L_c} + \boldsymbol{\gamma} \mathbf{I}_{sdq}^- \end{cases}$$

$$\begin{cases} \dot{\mathbf{V}}_{dq}^+ = \frac{\mathbf{I}_{sdq}^+ - \mathbf{I}_{dq}^+}{C_f} + \boldsymbol{\gamma} \mathbf{V}_{dq}^+ \\ \dot{\mathbf{V}}_{dq}^- = \frac{\mathbf{I}_{sdq}^- - \mathbf{I}_{dq}^-}{C_f} + \boldsymbol{\gamma} \mathbf{V}_{dq}^- \end{cases}$$

Linearization

$$\begin{cases} \Delta \mathbf{x} = [\Delta \mathbf{x}_{dq}^+ \quad \Delta \mathbf{x}_{dq}^- \quad \Delta \mathbf{x}_s \quad \Delta \mathbf{x}_{dc}]^T \\ \Delta \dot{\mathbf{x}} = \mathbf{A} \Delta \mathbf{x} + \mathbf{B} \Delta \mathbf{u} \end{cases}$$

$$\Delta \mathbf{x}_{dq}^+ = \left[\underbrace{\Delta \mathbf{I}_{sdq}^+ \quad \Delta \mathbf{V}_{dq}^+}_{\text{AC system}} \quad \underbrace{\Delta \mathbf{x}_{vdq}^+ \quad \Delta \mathbf{x}_{ldq}^+}_{\text{Inner control}} \right]^T$$

$$\Delta \mathbf{x}_{dq}^- = \left[\underbrace{\Delta \mathbf{I}_{sdq}^- \quad \Delta \mathbf{V}_{dq}^-}_{\text{AC system}} \quad \underbrace{\Delta \mathbf{x}_{vdq}^- \quad \Delta \mathbf{x}_{ldq}^-}_{\text{Inner control}} \right]^T$$

$$\Delta \mathbf{x}_{dc} = \left[\underbrace{\Delta I_{dc} \quad \Delta V_{dc}}_{\text{DC system}} \right]^T$$

GFM_{VSM}

$$\Delta \mathbf{x}_s = [\Delta \mathbf{x}_V^+ \quad \Delta \mathbf{x}_V^- \quad \Delta \theta \quad \Delta \omega \quad \Delta x_p]^T$$

$$\Delta \mathbf{u} = \left[\Delta \mathbf{I}_{dq}^+ \quad \Delta \mathbf{I}_{dq}^- \quad \underbrace{\Delta P_{set} \quad \Delta V_{set}}_{\text{VSM control input}} \right]^T$$

GFM_{droop}

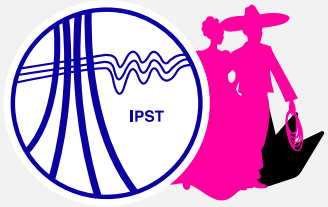
$$\Delta \mathbf{x}_s = [\Delta \mathbf{x}_V^+ \quad \Delta \mathbf{x}_V^- \quad \Delta \theta \quad \Delta x_p]^T$$

$$\Delta \mathbf{u} = \left[\Delta \mathbf{I}_{dq}^+ \quad \Delta \mathbf{I}_{dq}^- \quad \underbrace{\Delta P_{set} \quad \Delta V_{set}}_{\text{droop control input}} \right]^T$$

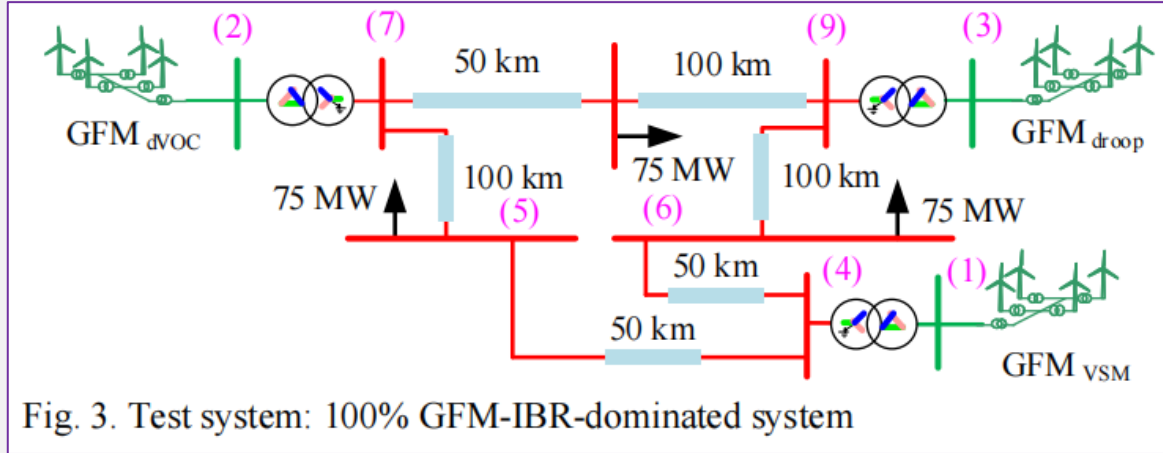
GFM_{dVOC}

$$\Delta \mathbf{x}_s = [\Delta \theta \quad \Delta V_d^* \quad \Delta x_p \quad \Delta x_Q]^T$$

$$\Delta \mathbf{u} = \left[\Delta \mathbf{I}_{dq}^+ \quad \Delta \mathbf{I}_{dq}^- \quad \underbrace{\Delta P_{set} \quad \Delta Q_{set} \quad \Delta V_{set}}_{\text{dVOC input}} \right]^T$$



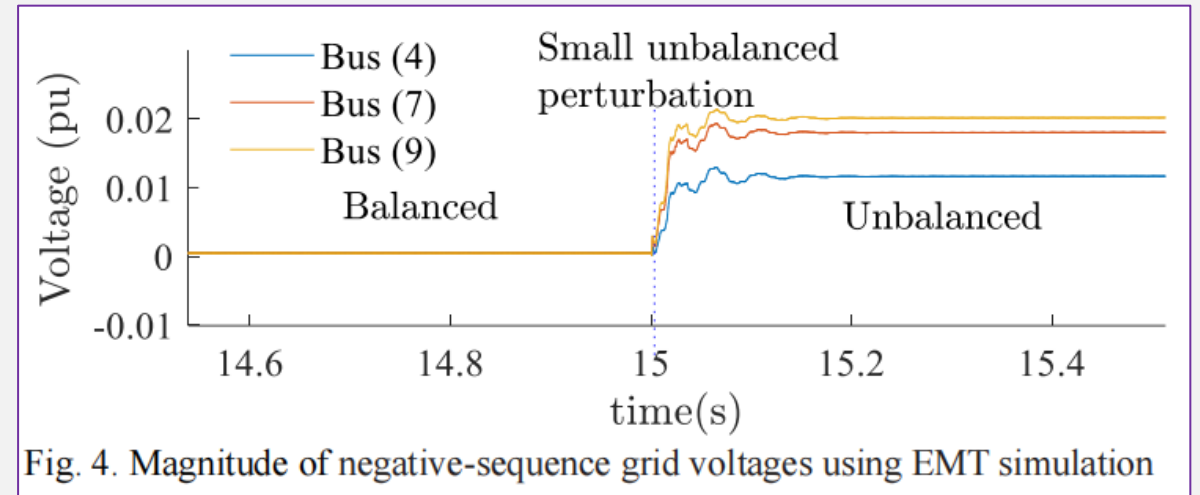
4. Dynamic model vs. EMT model

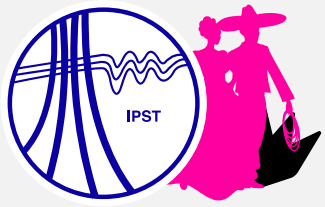


| TABLE AI PARAMETER CONFIGURATION OF GFM-IBRS | | | |
|---|--------------------------|------------------------|-----------------|
| Parameter | Value | Parameter | Value |
| N | 200 | (k_{pvac}, k_{ivac}) | (0.001, 0.0021) |
| (T_{dc}, k_{Vdc}) | (0.05 s, 0.83) | (k_{pv}, k_{iv}) | (0.52, 232.2) |
| ω_n | 314 rad/s | (k_{pi}, k_{ii}) | (0.73, 0.0059) |
| ω_f | 31.4 rad/s | (P_{set}, Q_{set}) | (1 pu, 0 pu) |
| (D_p, J) | (1.01e5, 2.02e3) | (V_{set}, V_{dcset}) | (1 pu, 2.45 kV) |
| (κ_1, κ_2) | (0.0209, 1.39e3) | m_p | 3.14e-8 |
| (R_c, L_c) | (5e-6 Ω , 1e-6 H) | (C_{dc}, C_f) | (1.6 F, 0.06 F) |
| T_{rm} | 230 kV / 13.8 kV | T_{ru} | 13.8 kV / 1 kV |

In test system, GFM-IBR operates at $P_m=75$ MW. For illustration, when $t=15$ s, a 75 MW unbalanced load is applied at Bus (6), resulting in the imbalance of grid voltages and currents.

The time step and simulation duration are set to 100 μ s and 20 s, respectively.





4. Dynamic model vs. EMT model

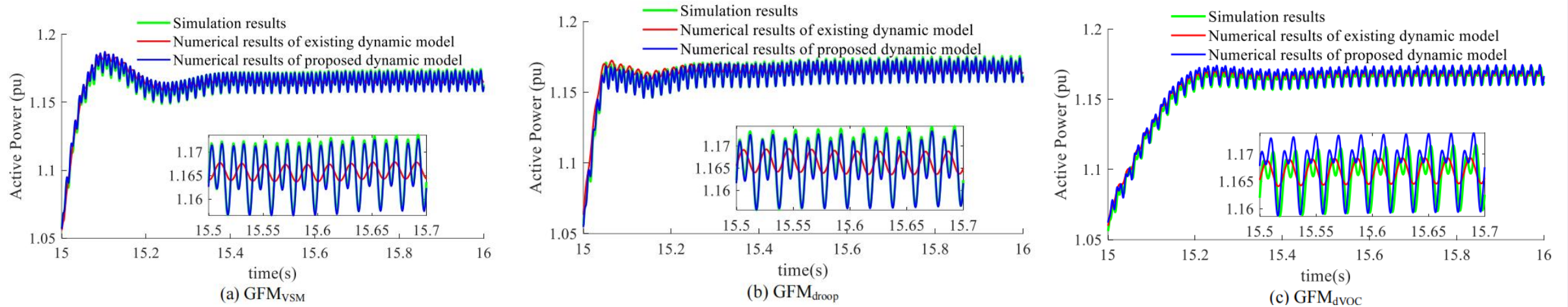


Fig. 5. Numerical results and EMT simulation results of active power responses of GFM-IBRs

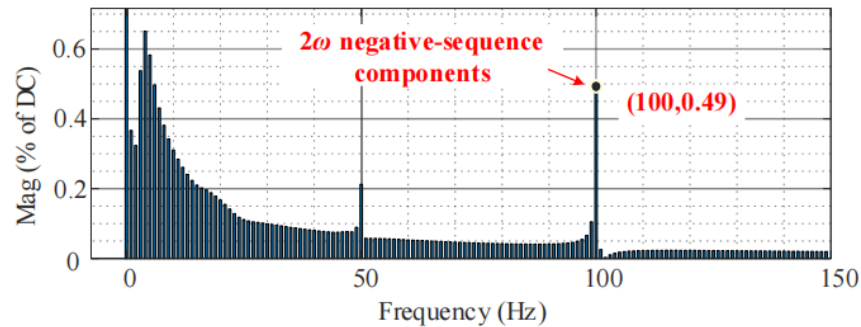
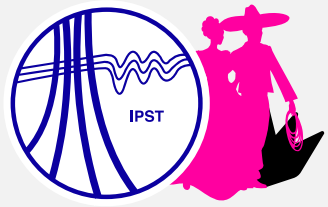


Fig. 6. FFT analysis based on EMT simulation results of active power response of GFM_{VSM}

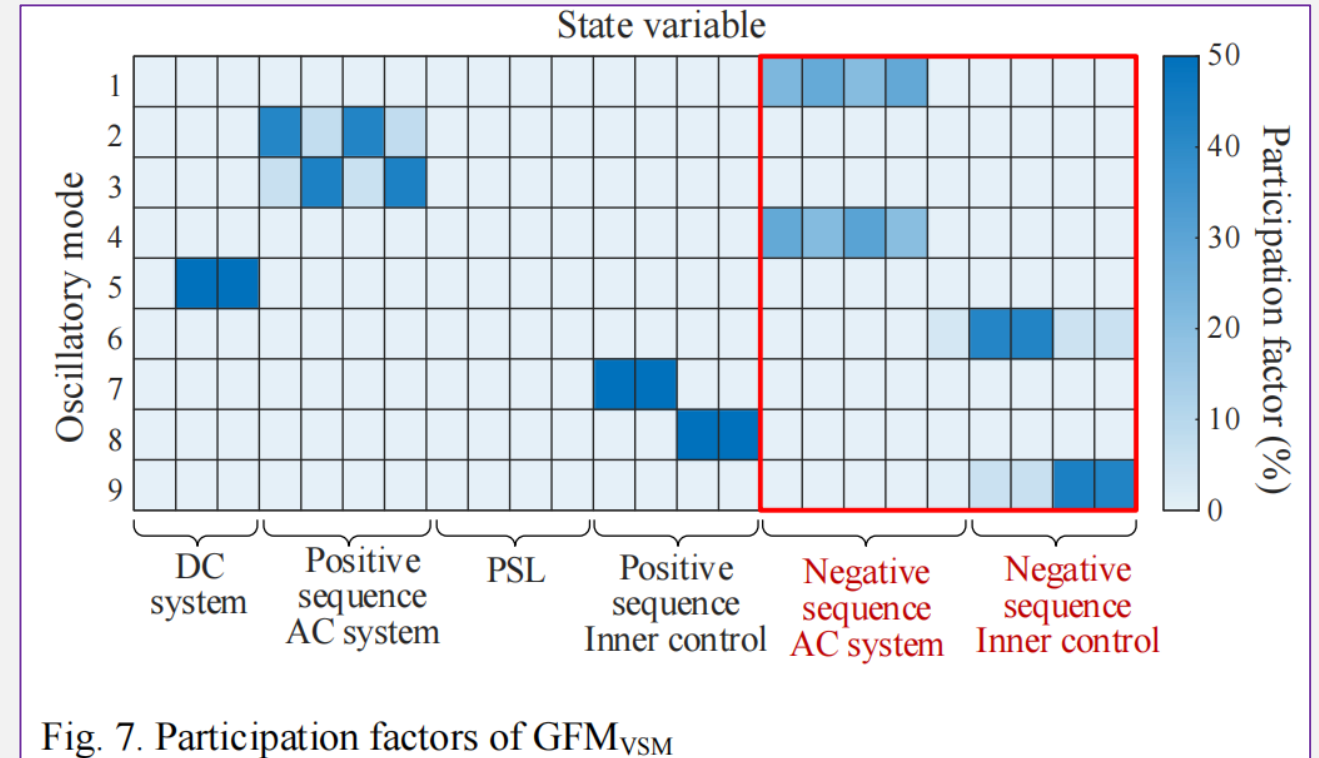
During the interval $t=15-15.2$ s, the transient dynamics of active power differ among GFM-IBRs due to each plant's different primary control strategies. Under steady-state unbalanced grid conditions, the dynamics of the proposed model are highly consistent with the EMT simulations. In addition, Fig. 6 shows that the 100% GFM-IBR-dominated system can still provide a path for the flow of 2ω negative-sequence components.

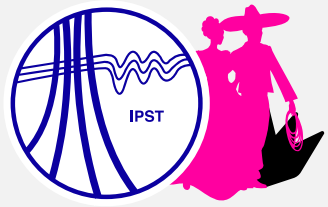


5. Modal Analysis and EMT Studies for GFM-IBRs

A. Oscillatory Modes of GFM-IBRs under Small Unbalanced Perturbations

Based on the state-space matrix derived from the proposed dynamic model, the eigenvalue-based stability assessment (EBSA) is used to study the impacts of control settings and negative-sequence control solutions on oscillatory modes dominated by 2ω negative-sequence components.





5. Modal Analysis and EMT Studies for GFM-IBRs

A. Oscillatory Modes of GFM-IBRs under Small Unbalanced Perturbations

TABLE I
OSCILLATORY MODES OF GFM_{VSM}

| Mode | λ | δ | f/Hz | Dominant Variables | |
|------|---------------|----------|---------------|--------------------|-------------------|
| 1 | -1719±2524i | 0.56 | 401.82 | ΔI_{sdq}^- | ΔV_{dq}^- |
| 2 | -1931±2264i | 0.65 | 360.45 | ΔI_{sd}^+ | ΔV_d^+ |
| 3 | -1763±1718i | 0.72 | 273.55 | ΔI_{sq}^+ | ΔV_q^+ |
| 4 | -1976±1457i | 0.80 | 231.89 | ΔI_{sdq}^- | ΔV_{dq}^- |
| 5 | -7.20±143.7i | 0.05 | 22.88 | ΔI_{dc} | ΔV_{dc} |
| 6 | -2.17±0.73i | 0.95 | 0.12 | Δx_{vdq}^- | |
| 7 | -2.23±0.0015i | 1.00000 | 0.00025 | Δx_{vdq}^+ | |
| 8 | -1.61±0.0007i | 1.00000 | 0.00012 | Δx_{Idq}^+ | |
| 9 | -1.53±0.0510i | 0.99945 | 0.00812 | Δx_{Idq}^- | |

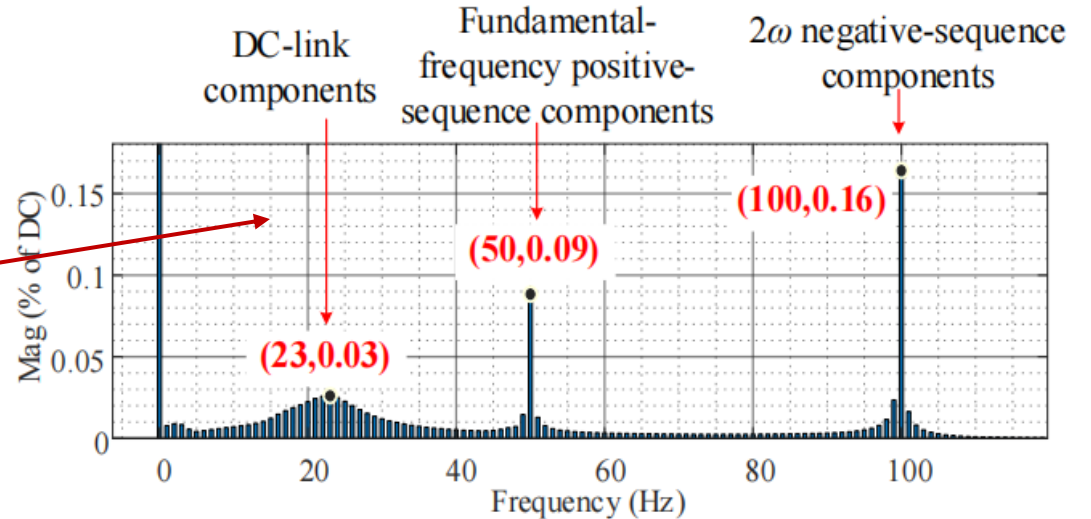
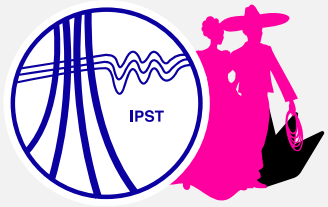


Fig. 8. FFT analysis based on EMT simulation results of the DC-link voltage under small, unbalanced perturbations

The 2ω negative-sequence components induce undesirable oscillations across various frequencies, substantially degrading system dynamic performance. This critical effect is often overlooked in conventional dynamic models that neglect negative-sequence components.



5. Modal Analysis and EMT Studies for GFM-IBRs

B. Impact of Negative-Sequence Control Solutions on Oscillatory Modes

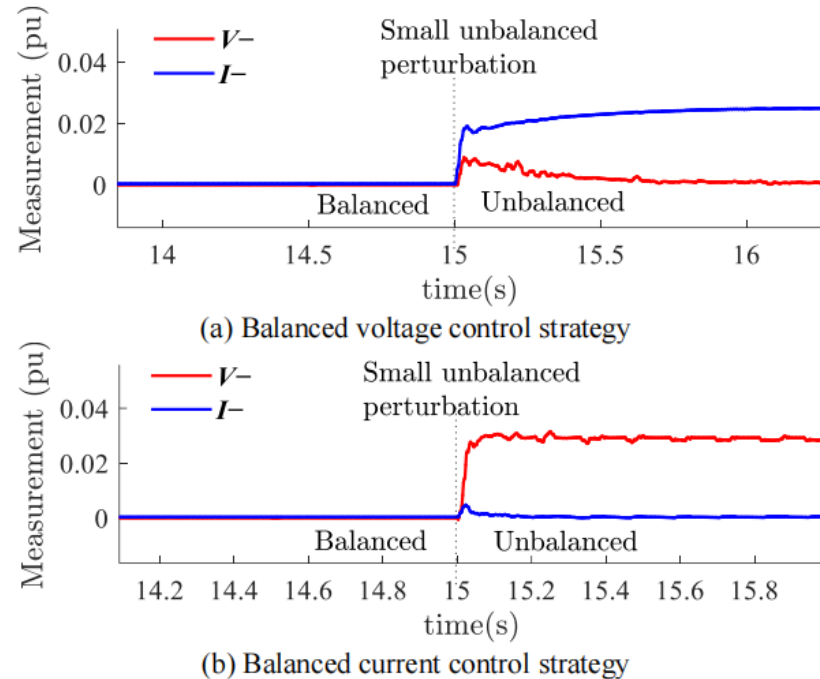


Fig. 9. EMT simulation results with negative-sequence control solutions in PNSC

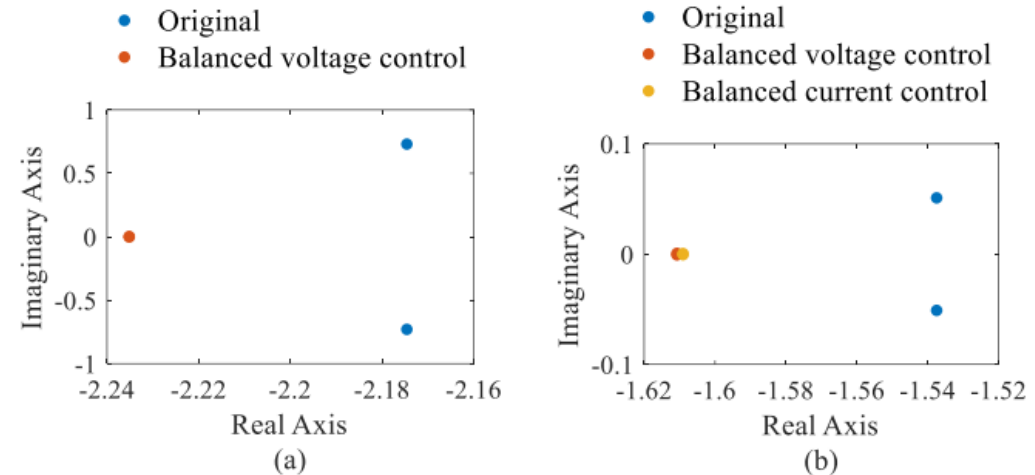
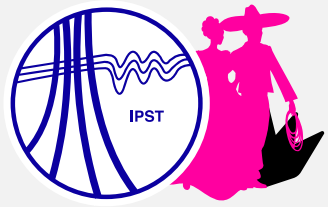


Fig. 10. Oscillatory modes dominated by negative-sequence components under BPSC and PNSC strategies: (a) Modes dominated by Δx_{Vdq}^- ; (b) Modes dominated by Δx_{Ida}^- .



The additional negative-sequence control solution can eliminate the oscillation, thus improving the control damping of GFM-IBRs.

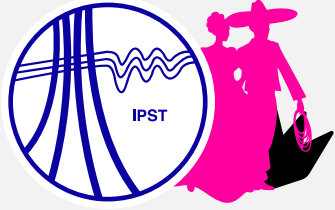


6. Conclusions

This paper introduces a novel generic decoupled-sequence dynamic model for GFM-IBRs, providing crucial insights into the behavior of 2ω negative-sequence components within the GFM BPSC system under small, unbalanced perturbations.

- 1. Impact of Negative Sequence Components:** The 2ω negative-sequence components induce undesirable oscillations across various frequencies, substantially degrading system dynamic performance. This critical effect is often overlooked in conventional dynamic models that neglect negative-sequence components.
- 2. Effectiveness of Negative-Sequence Control:** Implementing balanced current and voltage control strategies shifts oscillatory modes leftward and reduces their imaginary components to zero. This finding suggests the adoption of supplementary negative-sequence controls in GFM-IBRs to enhance control damping under small, unbalanced perturbations.

The proposed model and analysis method provide a powerful methodology for understanding and mitigating the impacts of negative-sequence behavior on system dynamics in GFM-IBR-dominated grids. While this study employs EBSA to focus on oscillatory mode analysis rather than instability mechanisms, it lays a foundation for future research.



IPST 2025
International Conference on
Power Systems Transients
Guadalajara, México.
8 to 12 June, 2025

Thank you!
Q&A

Prof. Ilhan Kocar
Polytechnique Montreal